Published in final edited form as:
J Mass Spectrom. 2014 March ; 49(3): 201–209. doi:10.1002/jms.3327.

Multiple-stage linear ion-trap with high resolution mass spectrometry towards complete structural characterization of phosphatidylethanolamines containing cyclopropane fatty acyl chain in *Leishmania infantum*

Fong-Fu Hsu[a,*], **F. Matthew Kuhlmann**[b,c], **John Turk**[a], and **Stephen M. Beverley**[c]

[a]Mass Spectrometry Resource, Division of Endocrinology, Diabetes, Metabolism and Lipid Research, USA

[b]Division of Infectious Diseases, Washington University School of Medicine, St. Louis, MO, 63110, USA

[c]Department of Molecular Microbiology, Washington University School of Medicine, St. Louis, MO, 63110, USA

Abstract

The structures of phosphatidylethanolamine (PE) in *Leishmania infantum* are unique in that they consist of a rare cyclopropane fatty acid (CFA) containing PE subfamily, including CFA-containing plasmalogen PE species. In this contribution, we applied multiple-stage linear ion-trap combined with high-resolution mass spectrometry to define the structures of PEs that were desorbed as $[M - H]^-$ and $[M - H + 2Li]^+$ ions by ESI, respectively. The structural information arising from MS^n on both the molecular species are complimentary, permitting complete determination of PE structures, including the identities of the fatty acid substituents and their location on the glycerol backbone, more importantly, the positions of the double bond(s) and of the cyclopropane chain of the fatty acid chain, directing to the realization of the CFA biosynthesis pathways that were reported previously. We also uncovered the presence of a minor dimethyl-PE subclass that has not been previously reported in *L. infantum*. This LIT MS^n mass spectrometric approach led to unambiguous identification of PE molecules including many isomers in complex mixture that would otherwise be very difficult to define using other analytical approaches.

Keywords

phosphatidylethanolamine; plasmenylethanolamine; cyclopropane fatty acids; linear ion-trap mass spectrometry; ESI; *Leishmania infantum*; *Leishmania major*

[*]Correspondence to: Fong-Fu Hsu, Mass Spectrometry Resource, Division of Endocrinology, Diabetes, Metabolism, and Lipid Research, Washington University School of Medicine, St. Louis, MO, 63110, USA. fhsu@im.wustl.edu.

Supporting information
Additional supporting information may be found in the online version of this article at the publisher's web-site.

Introduction

Leishmaniasis is caused by parasitic protozoa of the genus *Leishmania*, which are spread by the bite of phlebotomine sand flies. *Leishmania infantum* (*L. infantum*) (syn. *Leishmania chagasi*), an obligatory intracellular parasite of mammalian macrophages, is the major cause of zoonotic visceral leishmaniosis (ZVL) in human and canine leishmaniosis (CanL) in dogs. The infected dogs, both domestic and wild, are the principal reservoir for *L. infantum* and can be a threat to public health.[1,2]

In *Leishmania*, phospholipids (PLs) account for ~70% of total cellular lipids, including phosphatidylcholine (PC, 30–40%), phosphatidylethanolamine (PE, ~10%) and phosphatidylinositol (PI, ~10%).[3,4] While phosphatidylserine (PS) has been reported in several species by thin layer chromatography-based methods,[4–6] other studies based on mass spectrometry analysis failed to detect this lipid.[7–9] The PL anchors consist of 1,2-diacyl, 1-alkyl-2-acyl, 1-alkenyl-2-acyl (plasmalogens) or in some cases lyso-alkyl or lyso-acyl groups. Interestingly, the majority (80–90%) of PE in *L. major* belongs to plasmenylethanolamine (1-*O*-1′-alkenyl-2-acyl-phosphotidylethanolamine),[10,8,9] which is also more abundant than diacyl-PE in the procyclic and blood stream forms of *T. brucei*.[11–13] Plasmalogens have been implicated in signal transduction, membrane fusion and trafficking, oxidant and prostaglandin synthesis. Targeted *Leishmania* lacking the gene encoding alkyldihydroxyacetonephosphate synthase (ADS), the first committed step of ether lipid synthesis, lack all ether-linked lipids, yet remain viable with retention of significant animal infectivity.[9] However, the role of plasmenylethanolamine in *Leishmania* is not fully understood.

One interesting distinction in the PE contents among the various *Leishmania* species is the occurrence of cyclopropane fatty acids (CFAs) in *L. infantum*, *L. mexicana* and in *L. braziliensis*, while CFA-containing PEs are absent in *L. major* and in other kinetoplastids including *Trypanosoma*.[14] This lack of CFA-containing PEs in the latter species is attributable to the absence of the single gene encoding CFA synthetase (CFAS). This finding is supported by the notion that CFA is not detectable in wild type *L. major*, and expression of the *L. infantum* CFAS gene in *L. major* generates cyclopropanated fatty acids, suggesting that the substrate for this modification is present in *L. major*, despite the absence of the modifying enzyme.[15] The function of CFA in *Leishmania* is unclear. It is suggested that loss of CFAs may lead to irreversible changes in cell physiology that cannot be rescued by re-expression. Aberrant cyclopropanation in *L. major* also decreases parasite virulence but does not influence parasite tissue tropism.[15] In *Escherichia coli*, it is believed that CFA protects against acid shock and is involved in long-term survival of non-growing cells associated with environmental stresses.[16] Cyclopropanation is believed to play a role in the pathogenesis of *Mycobacterium tuberculosis*.[17]

The presence of PE in *Leishmania* has been reported. However, tandem mass spectrometric approaches toward complete structural characterization of this lipid class, in particular, the CFA-containing PE species in *L. infantum*, have not been previously described.[3,4,10] Here, we demonstrated the utility of multiple stage linear ion-trap with high resolution mass spectrometry in the structural determination of this unique lipid family, including the

identities of the fatty acyl groups and their position on the glycerol backbone, as well as the location of the unsaturated bond(s) or the cyclic chain on the fatty acyl chain,.

Materials and methods

Sample preparation

Leishmania major FV1 (MOHM/IL/80/Friedlin virulent clone 1), *L. infantum* (MCAN/ES/98/LLM-877) and CFAS expressing (+CFAS) *L. major* (the construction is described elsewhere) were grown in M199 with 10% FBS and supplements as described.[18] Total lipids were extracted using a modified Folch extraction[19] in which the water was replaced by an equal volume of 50 mM sodium fluoride. Cells ($2e^8$) were pelleted and resuspended in 1.5 ml 25 mM sodium fluoride. Methanol (2 ml) was added and the sample was sonicated for 20 s at full power using a Branson Sonifier 250 with a water bath attachment. Chloroform (4 ml) was added, and after vortexing for 30 s, the sample was centrifuged at 1800 × *g* for 15 min. The lower phase was removed and the upper phase was extracted again with 2.5 ml of chloroform:methanol (43:7). The sample was again vortexed and centrifuged. The combined lower phases were added with 2 ml of 50 mM sodium fluoride and 2 ml of methanol, vortexed and then centrifuged as above. The lower phase was dried by nitrogen stream and a final extraction with chloroform:methanol: 50 mM sodium fluoride (4:2:1) was performed with vortexing and centrifugation. The final lower phase was dried under nitrogen stream and resuspended in 1 ml of chloroform:methanol (1:1) for mass spectrometry analysis.

Mass spectrometry

Both high-resolution (R=100 000 at *m/z* 400) and low-energy CID tandem mass spectrometry experiments were conducted on a Thermo Scientific (San Jose, CA) LTQ Orbitrap Velos mass spectrometer (MS) with Xcalibur operating system. Lipid extracts in chloroform/methanol (2/1) were infused (1.5 μl/min) to the ESI source, where the skimmer was set at ground potential, the electrospray needle was set at 4.0 kV and temperature of the heated capillary was 300 °C. The automatic gain control of the ion trap was set to 5×10^4, with a maximum injection time of 50 ms. Helium was used as the buffer and collision gas at a pressure of 1×10^{-3} mbar (0.75 mTorr). The MS^n experiments were carried out with an optimized relative collision energy ranging from 25 to 45% and with an activation q value at 0.25, and the activation time at 10 ms to leave a minimal residual abundance of precursor ion (around 20%). The mass selection window for the precursor ions was set at 1 Da wide to admit the monoisotopic ion to the ion-trap for collision-induced dissociation (CID) for unit resolution detection in the ion-trap or high resolution accurate mass detection in the Orbitrap mass analyzer. Mass spectra were accumulated in the profile mode, typically for 3–10 min for MS^n spectra (n = 2, 3, 4).

Nomenclature

The abbreviations previously described for diacyl-, plasmanyl and plasmenyl (plasmalogen) PE were used.[20] The diacyl PE, for example, 1-palmitoyl-2-oleoyl-sn-glycero-3-phosphoethanolamine is abbreviated as 16:0/18:1-PE. The 1-O-alk-1′-enyl-2-acyl glycerophopholipids (*p*lasmalogens), for example, the 1-O-octadec-1′-enyl-2-oleoyl-*sn*-

glycero-3-phosphoethanolamine was designated as *p*18:0/18:1-PE, while dimethylphosphatidylethanolamine (DMPE), for example, 1-O-octadec-1′-enyl-2-linoleoyl-*sn*-glycero-3-phosphoethanol dimethylamine was designated as *p*18:0/18:2-DMPE. CFA such as 9,10-methyleneoctadecanoic acid was abbreviated as cPro(9) 19:1-fatty acid to reflect that the unsaturation on the C_{19}-chain is from the cyclopropane group at C-9. Thus, PE molecule consisting of cPro(9)19:1- and 18:0-fatty acyl groups at sn-1 and sn-2, respectively, is designated as cPro(9)19:1/18:0-PE.

Results and discussion

One unique feature of PE in *Leishmania* is that it mainly consists of plasmenylethanolamines (1-*O*-1′-alkenyl-2-acyl-phosphotidylethanolamine) rather than diacyl PEs.[10,8,9] As noted earlier, PE species are readily detectable as $[M - H]^-$ ions in the negative ion mode, when subjected to ESI. In the positive ion mode, ions in the fashions of $[M + Cat]^+$ and $[M - H + 2Cat]^+$ (Cat = H, Li, Na, K) are formed, dependent on the presence of alkali cations.[21,22] MS^n on the $[M - H]^-$ and lithiated ions yielded complementary structural information, leading to complete structural characterization.[21–24] The ion-trap MS^n mass spectrometric approaches with high resolution mass spectrometry toward characterization of this complex PE family from *L. Infantum* are described below.

Structural elucidation of the PE family of L. infantum as $[M - H]^-$ ions applying high resolution LIT MS^n (*n* = 1, 2, 3)

High resolution mass spectrometry (R = 100 000 at *m/z* 400) readily resolved isobaric ions, and the elemental compositions of the $[M - H]^-$ ions deduced from accurate mass measurements also readily differentiate a diacyl PE from a plasmalogen PE isolated from *L. infantum* (Table 1) (the corresponding ESI-MS spectrum is shown in the supplementary material Fig. s1a). For instance, two ions at *m/z* 714.5079 (calculated mass: 714.5079 Da; elemental composition: $C_{39}H_{73}O_8NP$) and 714.5442 (calculated mass: 714.5443; elemental composition: $C_{40}H_{77}O_7NP$), representing a diacyl-PE and plasmeny-PEs, respectively, were observed, and the latter species (38%) is more abundant than the former (12%) indicating that plasmenylethanolamines are the predominant species. High resolution MS^n on the $[M - H]^-$ ions further distinction of these two structures as described below.

As shown in Fig. 1a, the high resolution MS^2 spectrum of the $[M - H]^-$ ion at *m/z* 714 contained the ions at *m/z* 450 and 432 arising from losses of the 18:1-fatty acid substituent as a ketene and as an acid, respectively, consistent with the presence of the prominent ion at *m/z* 281, representing an 18:1-carboxylate anion (see supplemental material Table s1a). Further dissociation of the ion of *m/z* 450 (714 → 450; Fig. 1b) gave rise to ions at *m/z* 407 and 389, arising from losses of the ethanolamine group as aziridine and ethanolamine residues, respectively. The spectrum also contained the alkenoxide ion at *m/z* 253 ($^-O–CH=CHC_{15}H_{31}$), along with prominent ion at *m/z* 196 arising from loss of the 1-O-alk-1-enyl residue at *sn*-1 as an alcohol (loss of $HO–CH=CHC_{15}H_{31}$), and the ions at *m/z* 140 and 153, representing a phosphoethanolamine and a 2-hydroxy-1, 3-cyclophosphoric anions, respectively.[20] The results indicate the presence of a *p*17:0/18:1-PE. The structural assignments are also supported by high resolution mass measurements (see supplemental material Table s1b)

The spectrum (Fig. 1a) also contained ions at *m/z* 436 and 418, arising from losses of 19:1-fatty acid substituent as a ketene and an acid, respectively, and the ion at *m/z* 295, representing the 19:1-carboxylate anion (Table s1a). The high resolution MS^3 spectrum of the ion of *m/z* 436 (714 → 436; Fig. 1c) contained ions at *m/z* 393 and 375 arising from, again, losses of an aziridine and an ethanolamine groups, respectively, together with the prominent ion at *m/z* 196 arising from loss of the 1-O-alk-1-enyl residue at *sn*-1 as an alcohol (loss of HO–CH=CH$C_{14}H_{29}$), the alkenoxide ion at *m/z* 239 ($^-$O–CH=CH$C_{14}H_{29}$) and the ions at *m/z* 140 (phosphoethanolamine anion) and 153 (2-hydroxy-1, 3-cyclophosphoric anion) as seen earlier (Table s1c). These structural information led to the assignment of *p*16:0/19:1-PE; while assignment of the 19:1-fatty acid substituent as 9,10-methyleneoctadecanoic acid (cPro(9)19:1-FA) was further conducted by MS^n on the corresponding dilithiated ions (see below).

In Fig. 1a, ions at *m/z* 452 and 434 arising from losses of 18:2-fatty acid substituent as a ketene and as a fatty acid, along with ions at *m/z* 476 and 458 arising from the analogous losses of the 16:0-fatty acid substituent, are also present. The former ion pairs (i.e. ions at *m/z* 452 and 434) are, respectively, more abundant than the latter pairs, indicating the presence of 16:0/18:2-PE. The assignment of this latter isomer is consistent with the observation of the ion at *m/z* 279 (18:2-carboxylate anion), which is more abundant than the ion at *m/z* 255 (16:0-carboxylate anion), and further supported by the MS^3 spectrum of the ion at *m/z* 452 (714 → 452) as shown in Fig. 1d. The spectrum contained ions at *m/z* 409 (loss of aziridine) and 391 (loss of ethanolamine) arising from cleavages of the ethanol-amine head group and the abundant 16:0-carboxylate anion at *m/z* 255, signifying the presence of a diacyl-PE.[20] The spectrum also contained the 14:0-carboxylate anion at *m/z* 227 and the ions at *m/z* 224 and 242 arising from losses of 14:0-fatty acyl substituent as an acid and as a ketene, respectively, together with a minor ion at *m/z* 363 arising from loss of ethanoldimethylamine. The results indicate the presence of a minor 14:0/18:2-DMPE isomer.

High resolution mass spectrometry also readily resolved the ion pairs of *m/z* 742.5391 (calculated. mass: 742.5392 Da; elemental composition: $C_{41}H_{77}O_8NP$) and 742.5755 (calculated. mass: 742.5756 Da; elemental composition: $C_{42}H_{81}O_7NP$), deriving from a diacyl-PE and a plasmenyethanolamine, respectively (Table 1). High resolution MS^2 on the ion of *m/z* 742.5 (Fig. 2a) (Table s2a) also confirmed that ions at *m/z* 480 and 462 arose from losses of 18:2 fatty acid substituent as a ketene and as an acid, respectively, consistent with the presence of the 18:2-carboxylate anion at *m/z* 279. These ions were formed together with the ions at *m/z* 476 and 458, arising from the analogous losses of the 18:0-fatty acid substituent, and the 18:0-carboxylate anion at *m/z* 283. The former ion pairs (*m/z* 480 and 462) are, respectively, more abundant than the latter ions (*m/z* 476 and 458), indicating the presence of 18:0/18:2-PE. This assignment is further supported by MS^3 on the ion of *m/z* 480 (742 → 480; Fig. 2b), which yielded the prominent ions at *m/z* 283 (18:0-carboxylate anion) along with ions at *m/z* 419 (loss of ethanolamine) and 196 as seen earlier. The spectrum (Fig. 2b) also contained ions at *m/z* 391 corresponding to loss of an ethanoldimethylamine residue, together with the ions at *m/z* 255 (16:0-carboxylate anion)

and at *m/z* 224 arising from loss of 16:0-fatty acid substituent, suggesting the presence of 16:0/18:2-DMPE isomer (Table 1).

In Fig. 2a, ions at *m/z* 478 (loss of 18:1-ketene) and 460 (loss of 18:1-acid), together with ions at *m/z* 281 (18:1-carboxylate anion) are also present, indicating the presence of 18:1/18:1-PE. This structural assignment is also confirmed by the MS^3 spectrum of the ion of *m/z* 478 (742 → 478; data not shown), which is dominated by the ion of *m/z* 281, along with ions at *m/z* 417 (loss of ethanolamine) and 196, analogous to those seen in Fig. 1d and 2b.

The ion pairs of *m/z* 464 (measured: 464.3145; calculated *m/z* for $C_{23}H_{47}O_6NP$: 464.3146 Da) and 446 (measured: 446.3039; calculated *m/z* for $C_{23}H_{45}O_5NP$: 446.3041 Da) (Fig. 2a) arose from losses of a 19:1-fatty acid substituent as a ketene and as an acid, respectively, and consistent with the observation of the 19:1-carboxylate anion at *m/z* 295.2642 (calculated *m/z*: 295.2643; elemental composition: $C_{19}H_{35}O_2$) (Table s2a). The MS^3 spectrum of the ion at *m/z* 464 (742 → 464; Fig. 2c) contained ions at *m/z* 421 and 403 arising from cleavages of the ethanolamine head group and the abundant ions at *m/z* 267 ($^-O–CH=CHC_{16}H_{33}$), at *m/z* 196 (loss of $HO–CH=CHC_{16}H_{33}$), along with the common ions of *m/z* 153 and 140 as seen earlier. These structural assignments, again, were confirmed by high resolution mass measurements (see Table s2b). The profile of the spectrum is identical to that shown in Fig. 2b, indicating the presence of *p*18:0/cPro(9)19: 1-PE. Notably, ions at *m/z* 393 and 375, arising from losses of N, N-dimethylethyleneamine and N.N-dimethylethanolamine, respectively, are also present. The observation of these ions together with the phosphoethanoldimethylamine anion at *m/z* 168, the alkenoxide ion at *m/z* 239 ($^-O–CH=CHC_{14}H_{29}$) and the ion at *m/z* 224 (loss of $HO–CH=CHC_{14}H_{29}$) demonstrates the presence of a *p*16:0/cPro(9)19:1-DMPE isomer.

The above structural assignments neither provide distinction between a double bond and a cyclopropane chain, nor locate the positions of double bond(s) and of cyclopropane ring along the fatty acyl chain. However, LIT MS^n on the corresponding $[M – H + 2Li]^+$ adduct ions readily yield rich fragment ions for the structural identification, which is described below.

Characterization of PE from L. infantum as $[M – H + 2Li]^+$ ions by LIT MS^n (*n* = 1, 2, 3) mass spectrometry

The analogous $[M – H + 2Li]^+$ ions corresponding to the $[M – H]^-$ ions at *m/z* 714 were seen at *m/z* 728. MS^2 on the ion of *m/z* 728 (Fig. 3a) yielded ions at *m/z* 605 and 599 by losses of $(HO)O=P–O–CH_2CH_2(NH–)$ (123 Da) and $(LiO)(O=P)–O–CH_2CH_2(NH–)$ (129 Da) residues, respectively, via cleavage of the $CH_2O–P$ bond (see inset in Fig. 3a for the fragmentation processes) of the head group.[21] Further dissociation of the ion of *m/z* 605 (728 → 605; Fig. 3b) gave rise to ions at *m/z* 293 and 269, corresponding to the dilithiated ions of 18:2- and 16:0-FA, respectively, together with the ions of *m/z* 367 and 343 arising from losses of 16:0-ketene and 16:0-Li salt respectively, and the ions at *m/z* 343 and 319 arising from the analogous losses of 18:2-fatty acid substituent. The ions of *m/z* 367 and 343 are, respectively, more abundant than the ions of *m/z* 343 and 319, indicating that the 16:0- and 18:2-fatty acid substituents are located at sn-1 and sn-2, respectively,[24] consistent with

the presence of 16:0/18:2-PE. MS^3 on the ion of *m/z* 293 (728 → 605 → 293; Fig. 3c) gave rise to ions at *m/z* 237, 195 and 141, and the spectrum is identical to the LIT MS^2 spectrum of $\Delta^{9,12}$18:2.[25,23] The results gave assignment of the structure of 16:0/$\Delta^{9,12}$18:2-PE. In Fig. 3b, ions at *m/z* 341 (loss of 18:1-ketene), 317 (loss of 18:1-Li salt) and at *m/z* 295 (dilithiated 18:1) are also present, consistent with the presence of *p*17:0/18:1-PE isomer deduced from the $[M - H]^-$ ion as seen earlier. Further dissociation of the ions of *m/z* 295 (728 → 605 → 295; Fig. 3d)) gave rise to major ions at *m/z* 197, 141 and 99, and the spectrum is identical to the LIT MS^2 spectrum of the dilithiated $\Delta^9$18:1-fatty acid standard.[25] The combined information gave assignment of *p*17:0/$\Delta^9$18:1-PE. In the same spectrum (Fig. 3a), ions at *m/z* 327 and 303 arising from losses of 19:1-fatty acid substituent as a ketene and as a lithium salt, along with the ion at *m/z* 309 representing a dilithiated 19:1-FA ion, were also observed. The presence of 19:1-fatty acyl substituent is again consistent with the assignment of *p*16:0/19:1-PE isomer in the negative-ion mode. The MS^4 spectrum of the ions at *m/z* 309 (728 →605 →309; Fig. 3e) is identical to the MS^2 spectrum of 9,10-methyleneoctadecanoic acid standard (Fig. 3f), confirming the presence of a cyclopropane 19:1-FA (cPro(9)19:1) rather than a linear odd-chain monoenoic fatty acid. The results gave assignment of *p*16:0/cPro(9)19:1-PE.

Similarly, the $[M - H + 2Li]^+$ ion at *m/z* 756 is equivalent to the $[M - H]^-$ ions of *m/z* 742 (Fig. 2) and gave rise to ions of *m/z* 633 and 627 arising from elimination of the phosphoethanolamine head group (Fig. 4a). The MS^3 spectrum of the ion at *m/z* 633 (756 → 633; Fig. 4b) contained the ion pairs of *m/z* 371 (loss of 18:2-ketene) and 347 (loss of 18:2-Li), of 369 (loss of 18:1-ketene) and 345 (loss of 18:1-Li), of 367 (loss of 18:0-ketene) and 343 (loss of 18:0-Li) and of 355 (loss of 19:1-ketene) and 331 (loss of 19:1-Li), indicating the presence of 18:2-, 18:1-, 18:0-, 19:1-fatty acyl substituents, consistent with the observation of the dilithiated fatty acid ions at *m/z* 293 (18:2), 295 (18:1), 297 (18:0) and 309 (19:1), respectively. The MS^3 spectra of the ions at *m/z* 293, 295 and at 309 (data not shown) are identical to those shown in Fig. 3c, 3d and 3e, respectively. The results locate the positions of the double bond(s) and of the cyclopropane ring along the fatty acyl chain, leading to the identification of 18:0/$\Delta^{9,12}$18:2-PE, $\Delta^9$18:1/$\Delta^9$18:1-PE, and *p*18:0/cPro(9)19:1-PE isomers.

Characterization of PE isolated from CFAS expressing (+CFAS) L. major

To further understand the synthetic pathways underlying the cyclopropanation, we also probe the structures of the PE species isolated from +CFAS *L. major* (Table 2) (Fig. s1b) and *L. major* (mock) (Table 3) (Fig. s1c).

For example, high resolution mass spectrometry readily resolved the $[M - H]^-$ ions of *m/z* 740 arising from +CFAS *L. major* and gave the ion pairs at *m/z* 740.5241 (calculated *m/z* for $C_{41}H_{75}O_8NP$: 740.5236) and 740.5606 (calculated *m/z* for $C_{42}H_{79}O_7NP$) that represent a diacyl and 1-*O*-alkyl-2-acyl PE isomers, respectively (Table 2). This notion is supported by the MS^2 spectrum of the ions of *m/z* 740 (Fig. 5a), which contained multiple ion pairs at *m/z* 480 (loss of 18:3-ketene) and 462 (loss of 18:3-acid); at *m/z* 478 (loss of 18:2-ketene) and 460 (loss of 18:2-acid); at *m/z* 476 (loss of 18:1-ketene) and 458 (loss of 18:1-acid); at *m/z* 464 (loss of 19:2-ketene) and 446 (loss of 19:2-acid); at *m/z* 462 (loss of 19:1-ketene) and

444 (loss of 19:1-acid), indicating the presence of 18:3-, 18:2-, 18:1, 19:2- and 19:1-fatty acyl substituents. The results are consistent with the observation of the carboxylate anions at *m/z* 277 (18:3), 279 (18:2), 281 (18:1), 293 (19:2) and 295 (19:1). The MS^3 spectra of the ions of *m/z* 478, 476, 464 and of 462 (data not shown) are identical to those shown earlier, giving the assignment of the major isomeric structures of *p*18:0/19:2-, *p*18:1/19:1-, 18:1/18:2- and 18:0/18:3-PE. The spectrum (Fig. 5a) also contained the minor ions at *m/z* 502, arising from loss of 16:0-FA as ketene. MS^3 on the ion of *m/z* 502 (740 → 502; Fig. 5b) yielded the prominent 18:3-carboxylate anion of *m/z* 277, together with ions at *m/z* 224, arising from loss of 18:3-FA, and at *m/z* 413 arising from loss of ethanoldimethylamine residue, indicating the presence of a 16:0/18:3-DMPE. The spectrum (Fig. 5b) also contained the ions at *m/z* 305 (20:3-carboxylate anion) and 196 (loss of 20:3-FA), pointing to the presence of a minor 16:0/20:3-PE isomer.

The location of the unsaturated bonds along the fatty acid chain was again determined by MS^n on the corresponding $[M - H + 2Li]^+$ ions at *m/z* 754. The MS^2 spectrum of the ion of m/z 754 (Fig. 5c) contained ions at *m/z* 631 (loss of 123) and 625 (loss of 129), arising from elimination of the head group. Further dissociation of the ion of *m/z* 631 (754 → 631; Fig. 5d) yielded the ion pairs of *m/z* 371 (loss of 18:3-ketene) and 347 (loss of 18:3-Li), of *m/z* 369 (loss of 18:2-ketene) and 345 (loss of 18:2-Li), of 367 (loss of 18:1-ketene) and 343 (loss of 18:1-Li), of 355 (loss of 19:2-ketene) and 331 (loss of 19:2-Li) and of 353 (loss of 19:1-ketene) and 329 (loss of 19:1-Li), together with the dilithiated 18:2-, 18:1-, 18:0-, 19:2, 19:1-fatty acid ions at *m/z* 293, 295, 297, 307 and 309, respectively, indicating the presence of 18:2-, 18:1-, 18:0-, 19:2, 19:1-fatty acid substituents. The MS^4 spectra of the ions at *m/z* 293, 295 and of 309 are identical to those shown in Fig. 3c, 3d and 3e, respectively. These results gave assignment of *p*18:1/cPro(9)19:1-PE, $\Delta^9$18:1/$\Delta^{9,12}$18:2-PE, and 18:0/$\Delta^{9,12,15}$18:3-PE. The MS^4 spectrum of the ion of *m/z* 307 (754 → 631 → 307; Fig. 5e) contained ions at *m/z* 251, 209 and 141, suggesting that the ion represents a 9,10-methyleneoctadecen-12-oic acid (see Panel f for the fragmentation pathways). These results revealed the presence of *p*18:0/cPro (9)Δ^{12}19:2-PE.

The observation of the ions of *m/z* 740 that represent the major isomers of *p*18:0/cPro(9)Δ^{12}19:2-PE and *p*18:1/cPro(9)19:1-PE in +CFAS *L. major* (Table 2) is in accord with the notion that the prominent ion at *m/z* 726 in *L. major* (mock) (Table 3) represents both a *p*18:0/$\Delta^{9,12}$18:2-PE and a *p*18:1/$\Delta^9$18:1-PE. These results indicate that in +CFAS *L. major*, the formation of the *p*18:0/cPro(9)Δ^{12}19:2-PE and p18:1/cPro(9)19:1-PE arose from cyclopropanation of the cis C (9), C(10) double bonds of the unsaturated $\Delta^{9,12}$18:2 and $\Delta^9$18:1-FA substituents within the *p*18:0/$\Delta^{9,12}$18:2 and *p*18:1/$\Delta^9$18:1-PE molecules, respectively, via transfer of a methylene group. This is consistent with biosynthesis pathways of CFA-containing PE catalyzed by CFA synthase as previously described.[15] Similar cyclopropanations were evidenced in the entire PE family in +CFAS *L. major* (Table 2), in which the most notable was seen for the base ion of *m/z* 742 (100%), which represents a *p*18:0/cPro(9)19:1-PE arising from cyclopropanation of *p*18:0/$\Delta^9$18:1-PE, consistent with the observation of the base ion at *m/z* 728 (100%) representing a *p*18:0/$\Delta^9$18:1-PE in *L. major* (mock) (Table 3).

Conclusions

The utility of high resolution combined with multiple stage tandem mass spectrometry of a LIT Orbitrap permits structural identification of the complex PE family in mixtures, revealing the detailed structures including the identities of the fatty acid substituents and their location on the glycerol backbone, the positions of the cyclopropane group and/or of the unsaturated bond(s) along the fatty acyl chains of the various isomers in *L. infantum*, *L. major* (mock) and in +CFAS *L. major*. This study also supports the CFA biosynthesis pathways catalyzed by CFA synthase.

Supplementary Material

Refer to Web version on PubMed Central for supplementary material.

Acknowledgments

This research was supported by US Public Health Service Grants P41-GM103422, P60-DK-20579, P30-DK56341, RO1AI-31078 (SMB), and funds from the Department of Internal Medicine Washington University (FMK).

References

1. Podaliri Vulpiani M, Iannetti L, Paganico D, Iannino F, Ferri N. Methods of Control of the Leishmania infantum Dog Reservoir: State of the Art. Veterinary Medicine International. 2011
2. Gramiccia M, Gradoni L. The current status of zoonotic leishmaniases and approaches to disease control. Int J Parasitol. 2005; 35:1169–1180. [PubMed: 16162348]
3. Beach DH, Holz GGJ, Anekwe GE. Lipids of Leishmania promastigotes. J Parasitol. 1979; 65:201–216. [PubMed: 448607]
4. Wassef MK, Fioretti TB, Dwyer DM. Lipid analyses of isolated surface membranes of *Leishmania donovani* promastigotes. Lipids. 1985; 20:108–115. [PubMed: 3982233]
5. Ramos RG, Libong D, Rakotomanga M, Gaudin K, Loiseau PM, Chaminade P. Comparison between charged aerosol detection and light scattering detection for the analysis of Leishmania membrane phospholipids. J Chromatogr A. 2008; 1209:88–94. [PubMed: 18823632]
6. Yoneyama KAG, Tanaka AK, Silveira TGV, Takahashi HK, Straus AH. Characterization of Leishmania (Viannia) braziliensis membrane microdomains, and their role in macrophage infectivity. J Lipid Res. 2006; 47:2171–2178. [PubMed: 16861743]
7. Weingärtner A, Kemmer G, Müller FD, Zampieri RA, Gonzaga dos Santos M, Schiller J, Pomorski TG. *Leishmania* Promastigotes Lack Phosphatidylserine but Bind Annexin V upon Permeabilization or Miltefosine Treatment. PLoS ONE. 2012; 7:e42070. [PubMed: 22870283]
8. Zhang K, Showalter M, Revollo J, Hsu FF, Turk J, Beverley SM. Sphingolipids are essential for differentiation but not growth in Leishmania. EMBO J. 2003; 22:6016–6026. [PubMed: 14609948]
9. Zufferey R, Allen S, Barron T, Sullivan DR, Denny PW, Almeida IC, Smith DF, Turco SJ, Ferguson MAJ, Beverley SM. Ether Phospholipids and Glycosylinositolphospholipids Are Not Required for Amastigote Virulence or for Inhibition of Macrophage Activation by Leishmania major. Journal of Biological Chemistry. 2003; 278:44708–44718. [PubMed: 12944391]
10. Zhang K, Pompey JM, Hsu FF, Key P, Bandhuvula P, Saba JD, Turk J, Beverley SM. Redirection of sphingolipid metabolism toward de novo synthesis of ethanolamine in Leishmania. EMBO J. 2007; 26:1094–1104. [PubMed: 17290222]
11. Sutterwala SS, Hsu FF, Sevova ES, Schwartz KJ, Zhang K, Key P, Turk J, Beverley SM, Bangs JD. Developmentally regulated sphingolipid synthesis in African trypanosomes. Mol Microbiol. 2008; 70:281–296. [PubMed: 18699867]

12. Gibellini F, Hunter WN, Smith TK. The ethanolamine branch of the Kennedy pathway is essential in the bloodstream form of Trypanosoma brucei. Mol Microbiol. 2009; 73:826–843. [PubMed: 19555461]

13. Signorell A, Rauch M, Jelk J, Ferguson MAJ, Bütikofer P. Phosphatidylethanolamine in Trypanosoma brucei Is Organized in Two Separate Pools and Is Synthesized Exclusively by the Kennedy Pathway. J Biolog Chem. 2008; 283:23636–23644.

14. Peacock CS, Seeger K, Harris D, Murphy L, Ruiz JC, Quail MA, Peters N, Adlem E, Tivey A, Aslett M, Kerhornou A, Ivens A, Fraser A, Rajandream MA, Carver T, Norbertczak H, Chillingworth T, Hance Z, Jagels K, Moule S, Ormond D, Rutter S, Squares R, Whitehead S, Rabbinowitsch E, Arrowsmith C, White B, Thurston S, Bringaud F, Baldauf SL, Faulconbridge A, Jeffares D, Depledge DP, Oyola SO, Hilley JD, Brito LO, Tosi LRO, Barrell B, Cruz AK, Mottram JC, Smith DF, Berriman M. Comparative genomic analysis of three Leishmania species that cause diverse human disease. Nat Genet. 2007; 39:839–847. [PubMed: 17572675]

15. Oyola SO, Evans KJ, Smith TK, Smith BA, Hilley JD, Mottram JC, Kaye PM, Smith DF. Functional Analysis of *Leishmania* Cyclopropane Fatty Acid Synthetase. PLoS ONE. 2012; 7:e51300. [PubMed: 23251490]

16. Grogan DW, Cronan JE. Cyclopropane ring formation in membrane lipids of bacteria. Microbiol Mol Biol Rev. 1997; 61:429–41. [PubMed: 9409147]

17. Glickman MS, Cox JS, Jacobs WR Jr. A Novel Mycolic Acid Cyclopropane Synthetase Is Required for Cording, Persistence, and Virulence of Mycobacterium tuberculosis. Mol Cell. 2000; 5:717–727. [PubMed: 10882107]

18. Kapler GM, Coburn CM, Beverley SM. Stable transfection of the human parasite Leishmania major delineates a 30-kilobase region sufficient for extrachromosomal replication and expression. Mol Cell Biol. 1990; 10:1084–94. [PubMed: 2304458]

19. Folch J, Lees M, Sloane Stanley GH. A simple method for the isolation and purification of total lipides from animal tissues. J Biol Chem. 1957; 226:497–509. [PubMed: 13428781]

20. Hsu FF, Turk J. Differentiation of 1-O-alk-1′-enyl-2-acyl and 1-O-alkyl-2-acyl Glycerophospholipids by Multiple-Stage Linear Ion-Trap Mass Spectrometry with Electrospray Ionization. J Am Soc Mass Spect. 2007; 18:2065–2073.

21. Hsu FF, Turk J. Characterization of phosphatidylethanolamine as a lithiated adduct by triple quadrupole tandem mass spectrometry with electrospray ionization. J Mass Spectrom. 2000; 35:595–606. [PubMed: 10800048]

22. Hsu FF, Turk J. Charge-remote and charge-driven fragmentation processes in diacyl glycerophosphoethanolamine upon low-energy collisional activation: A mechanistic proposal. J Am Soc Mass Spect. 2000; 11:892–899.

23. Hsu FF, Turk J. Structural characterization of unsaturated glycerophospholipids by multiple-stage linear ion-trap mass spectrometry with electrospray ionization. J Am Soc Mass Spect. 2008; 19:1681–1691.

24. Hsu FF, Turk J. Electrospray ionization with low-energy collisionally activated dissociation tandem mass spectrometry of glycerophospholipids: Mechanisms of fragmentation and structural characterization. J Chromatogr B. 2009; 877:2673–2695.

25. Hsu FF, Turk J. Elucidation of the double-bond position of long-chain unsaturated fatty acids by multiple-stage linear ion-trap mass spectrometry with electrospray ionization. J Am Soc Mass Spect. 2008; 19:1673–1680.

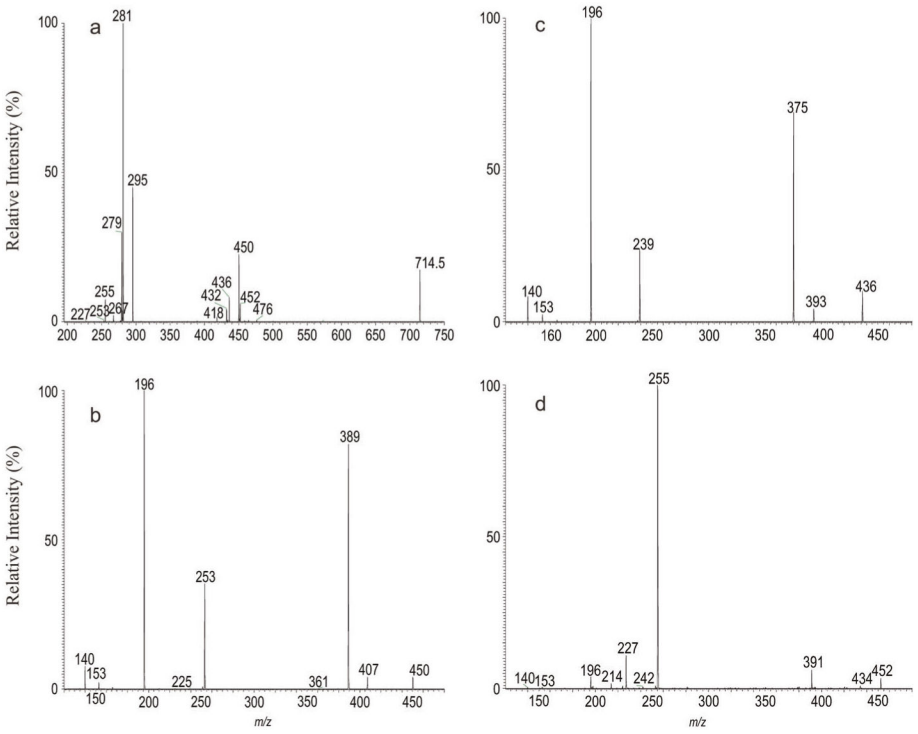

Figure 1.

The MS^2 mass spectrum of the $[M - H]^-$ ion of *m/z* 714.5 (a), its MS^3 spectra of the ions of *m/z* 450 (714 →450) (b), of *m/z* 436 (714 →436) (c) and of *m/z* 452 (714 → 452) (d).

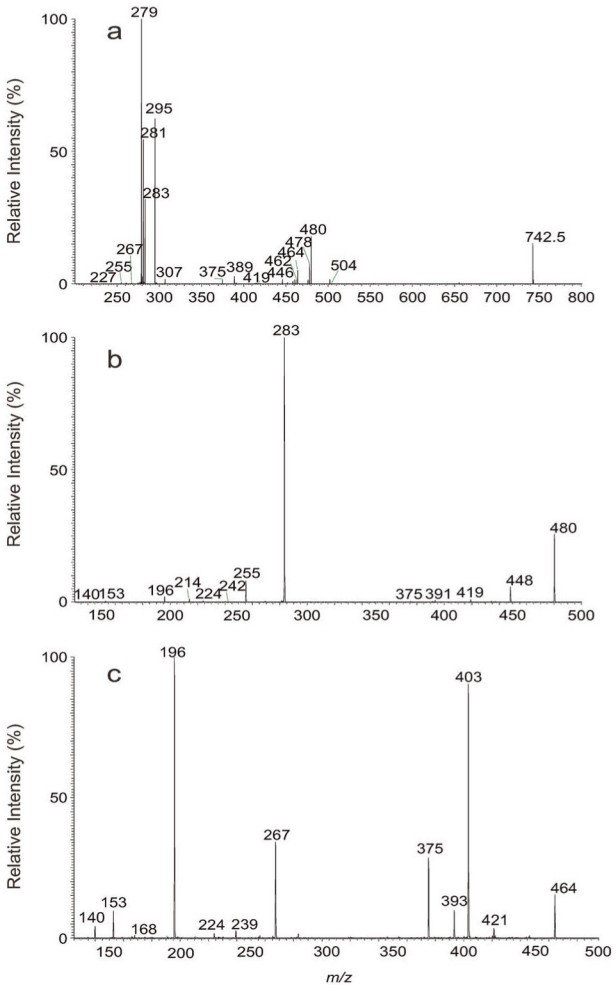

Figure 2.

The MS^2 mass spectrum of the $[M - H]^-$ ion of *m/z* 742.5 (a), its MS^3 spectra of the ions of *m/z* 480 (742 → 480) (b) and of *m/z* 464 (742 → 464) (c).

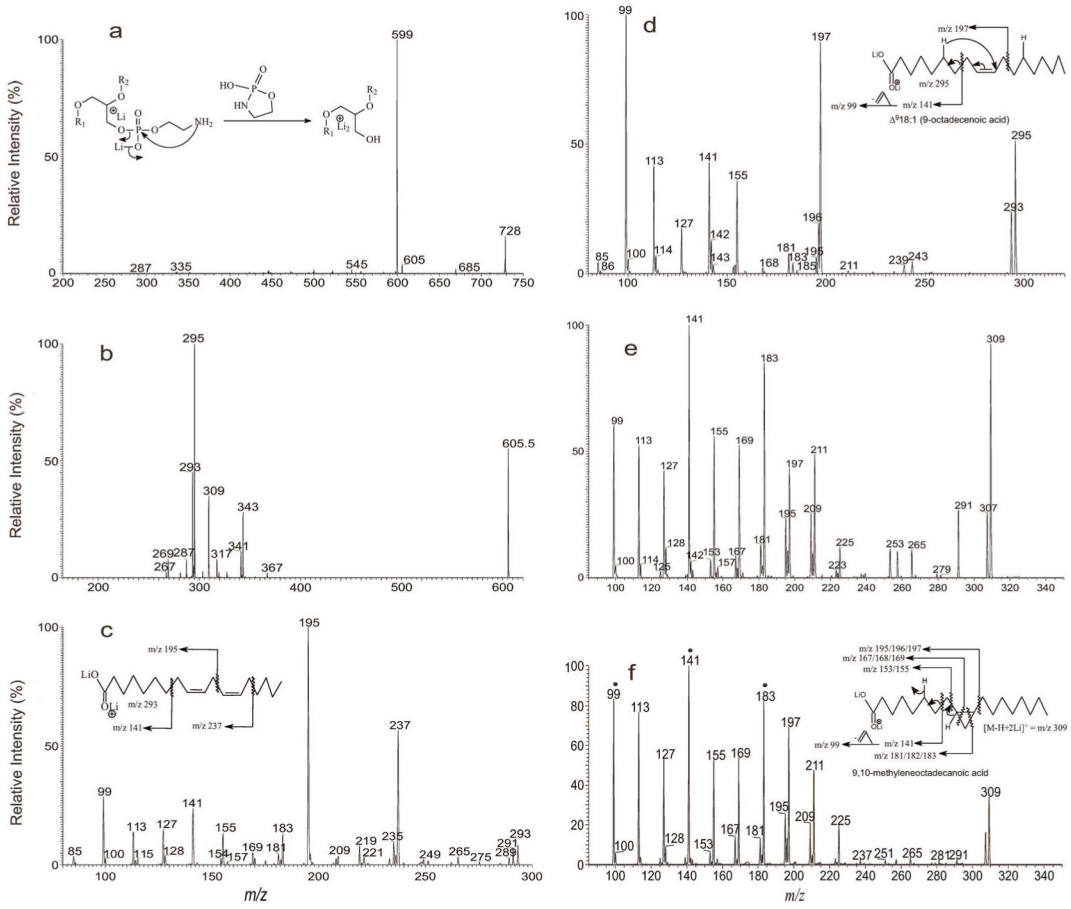

Figure 3.

The MS^2 mass spectrum of the $[M – H + 2Li]^+$ ion of *m/z* 728 (a), its MS^3 spectra of the ions of *m/z* 605 (728 →605) (b) and the MS^4 spectra of the ions of *m/z* 293 (728 →605 →293) (c), of *m/z* 295 (728 →605 →295) (d) and of *m/z* 309 (728 →605 →309) (e). The MS^2 mass spectrum of the $[M – H + 2Li]^+$ ion of 9,10-methyleneoctadecanoic acid standard at *m/z* 309 is shown in Panel f, which is similar to Panel e and gives the structural assignment. Shown in insets of Panels a, c, d and f are the proposed fragmentation pathways leading to locate the positions of double bond and/or of cycopropane group.

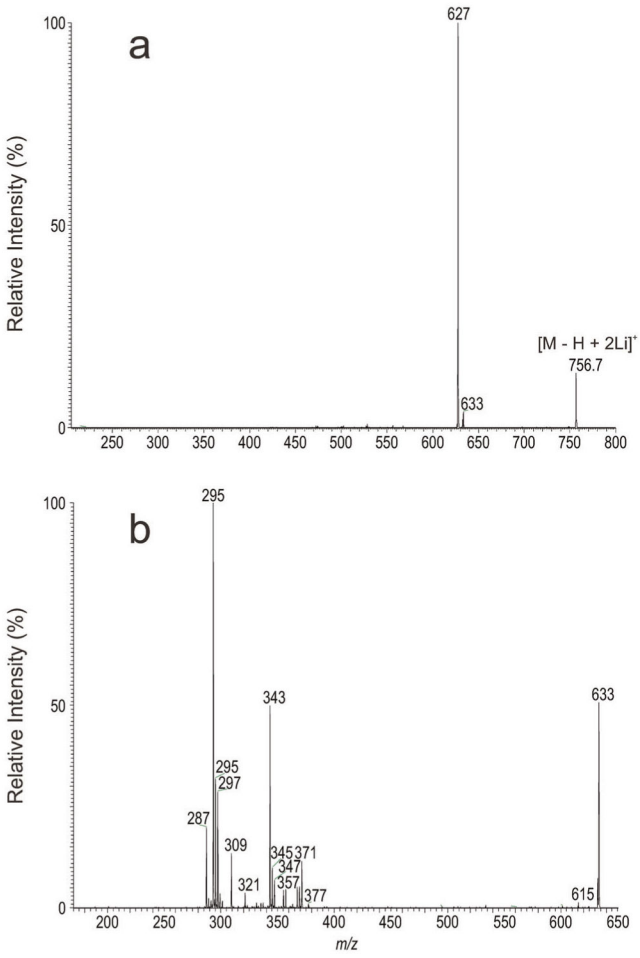

Figure 4.

The MS^2 mass spectrum of the $[M – H + 2Li]^+$ ion of *m/z* 756.7 (a) and its MS^3 spectra of the ions of *m/z* 633 (756 → 633) (b).

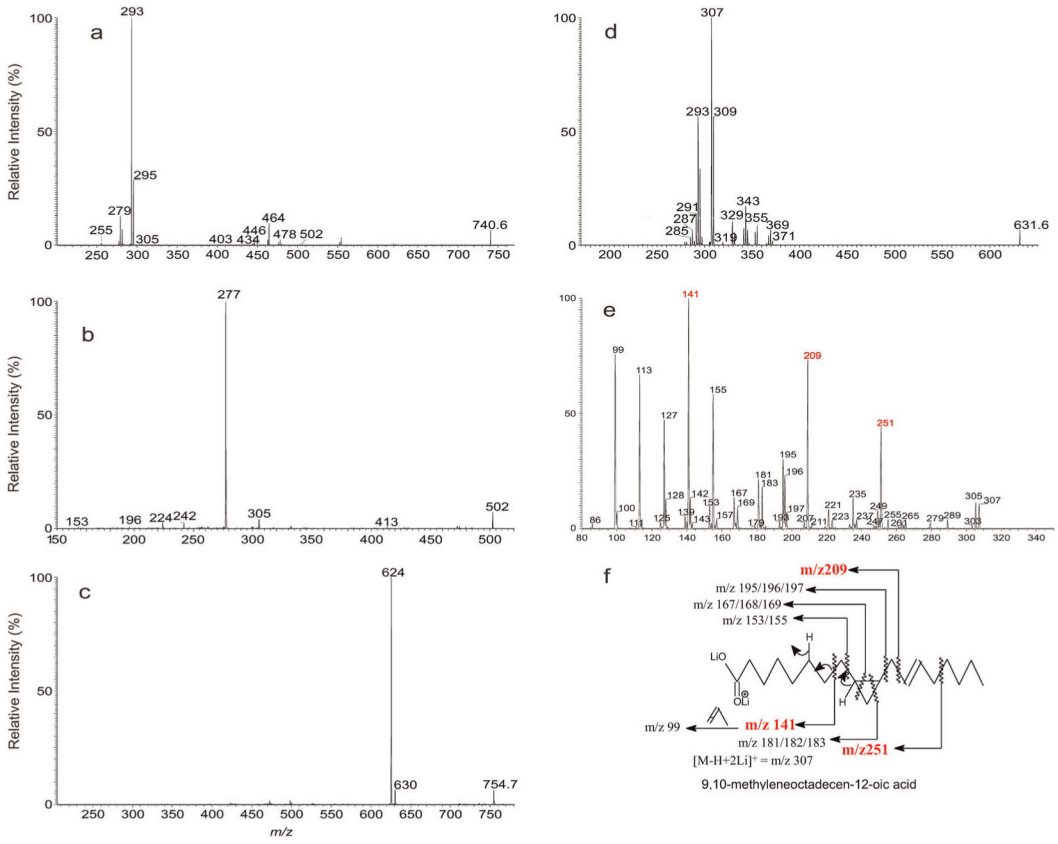

Figure 5.

The MS^2 mass spectrum of the $[M - H]^-$ ion of *m/z* 740.5 (a), its MS^3 spectra of the ions of *m/z* 502 (740 →502) (b) and the MS^2 mass spectrum of the corresponding $[M - H + 2Li]^+$ ion of *m/z* 754.7 (c), its MS^3 spectra of the ions of *m/z* 631 (754 →631) (d) and the MS^4 spectra of the ions of *m/z* 307 (754 → 631 → 307) (e). Panel (f) illustrates the fragmentation pathways leading to locate the double bond and cyclopropane group along the fatty acid chain.

Table 1

High resolution and LIT MS^n analysis of the structures of phosphatidylethanolamine isolated from *L. infantum*

Measured m/z $[M - H]^-$	Calcd. mass (Da)	Deviation (mDa)	Rel. int. (%)	Composition	[a] Structures
686.4766	686.4766	−0.06	4.93	C37 H69 O8 N P	14:0/18:2; 16:1/16:1
688.4922	688.4923	−0.08	3.98	C37 H71 O8 N P	14:0/18:1; 16:0/16:1
696.4973	696.4974	−0.07	3.41	C39 H71 O7 N P	p16:0/18:3
698.5130	698.5130	0.00	95.20	C39 H73 O7 N P	p16:0/$\Delta^{9,12}$18:2
700.5286	700.5287	−0.07	100.00	C39 H75 O7 N P	p16:0/Δ^{9}18:1
712.4922	712.4923	−0.06	4.76	C39 H71 O8 N P	16:0/18:3
712.5287	712.5287	0.05	23.24	C40 H75 O7 N P	p16:0/cPro(9) Δ^{12}19:2
714.5079	714.5079	−0.06	11.71	C39 H73 O8 N P	16:0/18:2; 16:1/18:1; 14:0/18:2-DMPE
714.5442	714.5443	−0.07	38.45	C40 H77 O7 N P	p17:0/18:1; p16:0/cPro(9)19:1
716.5235	716.5236	−0.10	7.86	C39 H75 O8 N P	16:0/18:1
724.5286	724.5287	−0.08	11.88	C41 H75 O7 N P	p18:1/$\Delta^{9,12}$18:2
726.5079	726.5079	0.01	4.23	C40 H73 O8 N P	17:0/18:3
726.5442	726.5443	−0.09	72.32	C41 H77 O7 N P	p18:0/$\Delta^{9,12}$18:2; p18:1/18:1; p16:0/$\Delta^{9,12}$18:2-DMPE
728.5234	728.5236	−0.20	5.49	C40 H75 O8 N P	17:0/18:2
728.5598	728.5600	−0.18	55.49	C41 H79 O7 N P	p18:0/Δ^{9}18:1; a18:1/Δ^{9}18:1; p17:0/cPro(9)19:1
730.5392	730.5392	−0.05	2.18	C40 H77 O8 N P	17:0/18:1
734.4763	734.4766	−0.32	2.25	C41 H69 O8 N P	18:3/18:3
736.4922	736.4923	−0.10	4.69	C41 H71 O8 N P	18:3/18:2
738.5078	738.5079	−0.09	7.34	C41 H73 O8 N P	18:3/18:1; 18:2/18:2; 16:0/20:4
740.5236	740.5236	−0.02	12.68	C41 H75 O8 N P	Δ^{9}18:1/$\Delta^{9,12}$18:2; 18:0/$\Delta^{9,12,15}$18:3; 16:0/20:3
740.5598	740.5600	−0.11	1.30	C42 H79 O7 N P	p18:1/19:1
742.5391	742.5392	−0.13	19.30	C41 H77 O8 N P	18:0/$\Delta^{9,12}$18:2; Δ^{9}18:1/Δ^{9}18:1; 16:0/$\Delta^{9,12}$18:2-DMPE; 16:0/20:2
742.5755	742.5756	−0.11	3.55	C42 H81 O7 N P	p18:0/19:1; p16:0/19:1-DMPE
744.5546	744.5549	−0.23	9.03	C41 H79 O8 N P	18:0/18:1
754.5392	754.5392	−0.07	3.12	C42 H77 O8 N P	18:2/19:1
756.5546	756.5549	−0.30	3.20	C42 H79 O8 N P	18:1/19:1; 19:0/18:2

[a] Unless indicated, the location of cyclopropane and unsaturated bond(s) is not determined.

Table 2

High resolution and LIT MS^n analysis of the structures of phosphatidylamine isolated from +CFAS *L. major*

Measured m/z [M - H]$^-$	Calcd. mass (Da)	Deviat. (mDa)	Rel. int. (%)	Composition	[a] Structures
686.4770	686.4766	0.36	2.53	C37 H69 O8 N P	14:0/18:2; 16:1/16:1
688.4927	688.4923	0.38	2.63	C37 H71 O8 N P	16:0/16:1; 14:0/$\Delta^9$18:1
698.5134	698.5130	0.37	1.41	C39 H73 O7 N P	p16:0/18:2
700.5291	700.5287	0.42	1.06	C39 H75 O7 N P	p15:0/19:1
712.5291	712.5287	0.44	2.16	C40 H75 O7 N P	p16:0/19:2
714.5084	714.5079	0.49	3.60	C39 H73 O8 N P	16:0/18:2; 18:1/16:1; 14:0/18:2-DMPE
714.5448	714.5443	0.50	13.22	C40 H77 O7 N P	p16:0/cPro(9)19:1
716.5240	716.5236	0.38	2.67	C39 H75 O8 N P	16:0/18:1
726.5448	726.5443	0.48	15.45	C41 H77 O7 N P	p18:0/$\Delta^{9,12}$18:2; p17:0/cPro(9) Δ^{12}19:2
728.5604	728.5600	0.47	11.54	C41 H79 O7 N P	p17:0/cPro(9)19:1; p18:0/$\Delta^9$18:1; a18:0/$\Delta^{9,12}$18:2; p15:0/19:1-DMPE
730.5398	730.5392	0.56	2.09	C40 H77 O8 N P	16:0/19:1
730.5760	730.5756	0.38	2.24	C41 H81 O7 N P	a18:0/18:1
736.4928	736.4923	0.53	1.33	C41 H71 O8 N P	18:3/18:2
738.5084	738.5079	0.49	2.30	C41 H73 O8 N P	18:1/18:3; 18:2/18:2; 16:1/18:3-DMPE; 16:0/20:4
738.5448	738.5443	0.49	2.50	C42 H77 O7 N P	p18:1/19:2
740.5241	740.5236	0.51	4.80	C41 H75 O8 N P	18:1/18:2; 18:0/18:3; 16:0/18:3-DMPE; 16:0/20:3
740.5604	740.5600	0.47	16.33	C42 H79 O7 N P	p18:0/cPro(9) Δ^{12}19:2; p18:1/cPro(9)19:1
742.5399	742.5392	0.69	9.54	C41 H77 O8 N P	18:0/18:2; 18:1/18:1
742.5759	742.5756	0.24	100.00	C42 H81 O7 N P	p18:0/cPro(9)19:1 + p16:0/cPro(9)19:1-DMPE
744.5553	744.5549	0.42	6.61	C41 H79 O8 N P	18:0/18:1
754.5396	754.5392	0.36	1.30	C42 H77 O8 N P	18:2/19:1; 18:1/19:2
754.5761	754.5756	0.44	1.07	C43 H81 O7 N P	p18:0/18:2-DMPE
756.5552	756.5549	0.35	2.86	C42 H79 O8 N P	18:1/19:1; 19:0/18:2
756.5916	756.5913	0.32	1.78	C43 H83 O7 N P	p18:0/20:1
758.5708	758.5705	0.31	3.56	C42 H81 O8 N P	16:0/19:1-DMPE; 18:0/19:1

[a] Unless indicated, the location of cyclopropane and unsaturated bond(s) is not determined.

Table 3

High resolution and LIT MS^n analysis of the structures of phosphatidylamine isolated from *L. major (mock)*

Measured m/z $[M - H]^-$	Calcd. mass (Da)	Deviat. (mDa)	Rel. int. (%)	Composition	[a] Structures
686.4769	686.4766	0.30	2.00	C37 H69 O8 N P	16:1/16:1
688.4925	688.4923	0.22	3.30	C37 H71 O8 N P	16:0/16:1
696.4977	696.4974	0.32	0.82	C39 H71 O7 N P	p16:0/18:3; p16:1/18:2
698.5133	698.5130	0.31	8.08	C39 H73 O7 N P	p16:0/18:2
700.5290	700.5287	0.30	17.70	C39 H75 O7 N P	p16:0/18:1; p18:0/16:1
712.4926	712.4923	0.30	0.94	C39 H71 O8 N P	16:1/18:2; 16:0/18:3
712.5290	712.5287	0.31	4.97	C40 H75 O7 N P	p17:0/18:2
714.5082	714.5079	0.32	3.88	C39 H73 O8 N P	16:0/18:2; 16:1/18:1
714.5446	714.5443	0.30	11.50	C40 H77 O7 N P	p17:0/18:1; p18:0/17:1
716.5239	716.5236	0.28	4.75	C39 H75 O8 N P	16:0/18:1
724.5290	724.5287	0.35	5.67	C41 H75 O7 N P	p18:1/$\Delta^{9,12}$18:2; p18:0/$\Delta^{9,12,15}$18:3
726.5447	726.5443	0.34	52.96	C41 H77 O7 N P	p18:0/$\Delta^{9,12}$18:2; p18:1/Δ^{9}18:2
728.5601	728.5600	0.17	100.00	C41 H79 O7 N P	p18:0/Δ^{9}18:1
736.4925	736.4923	0.20	1.36	C41 H71 O8 N P	18:3/18:2; 18:4/18:1; 14:0/22:5, 16:1/20:4
738.5081	738.5079	0.19	2.34	C41 H73 O8 N P	18:3/18:1; 18:2/18:2; 16:0/20:4
740.5238	740.5236	0.24	6.66	C41 H75 O8 N P	18:1/18:2; 18:0/18:3; 16:0/20:3
740.5604	740.5600	0.48	1.54	C42 H79 O7 N P	p18:0/19:2
742.5395	742.5392	0.31	12.53	C41 H77 O8 N P	18:0/$\Delta^{9,12}$18:2; Δ^{9}18:1/Δ^{9}18:1
742.5762	742.5756	0.56	2.86	C42 H81 O7 N P	p18:0/19:1
744.5551	744.5549	0.26	10.60	C41 H79 O8 N P	18:0/18:1
754.5395	754.5392	0.30	1.84	C42 H77 O8 N P	[b] 19:1/18:2
756.5552	756.5549	0.32	3.57	C42 H79 O8 N P	[b] 19:1/18:1

[a] Unless indicated, the location of cyclopropane and unsaturated bond(s) is not determined;

[b] sn-position not clear